Generation and Optimization of Femtosecond Pulses by Four-Wave Mixing Process

Takayoshi Kobayashi, Jun Liu, and Yuichiro Kida

(Invited Paper)

***Abstract*—Four-wave mixing (FWM) was used to generate and optimize ultrashort pulses with wavelengths from ultraviolet (UV) to near-infrared in bulk media and gases. Wavelength-tunable multicolored pulses were simultaneously generated by cascaded FWM in glass plates. By using incident chirped pulses, 15-fs self-compressed multicolored pulses were obtained with excellent properties. Self-compression was also used to generate ultrashort deep-UV (DUV) pulses. The positive frequency chirp in a self-phase-modulated pulseissuitable for this objective. Sub-10-fs DUV pulses were generated without using any additional pulse compressors. Self-diffraction was used to clean the pulse, broaden the spectrum, and enhance the spatial beam quality. These multicolored pulses can be simultaneously amplified and compressed by a four-wave optical parametric amplifier. The generated multicolored pulses are useful for multicolored ultrafast spectroscopy, microscopy experiments, and as seeds for petawatt lasers with high temporal contrasts.**

***Index Terms*—Nonlinear optics, optical pulse generation, spectroscopy, ultrafast optics, ultraviolet generation.**

Manuscript received October 14, 2010; revised December 27, 2010; accepted January 3, 2011. Date of publication February 17, 2011; date of current version January 31, 2012. This work was supported in part by the 21st Century Center of Excellence (COE) program on "Coherent Optical Science" and in part by a grant from the Ministry of Education (MOE), Taiwan under the Aiming Top University project Program at National Chiao Tung University. A part of this work was performed under the joint research project of the Laser Engineering, Osaka University, under contract subject B1-27. The work of J. Liu was supported by the opening funds from the State Key Laboratory of High-field Laser Physics, China.

T. Kobayashi is with the Advanced Ultrafast Laser Research Center and Department of Engineering Science, Faculty of Informatics and Engineering, The University of Electro-Communications, Chofu-shi, Tokyo 182-8585, Japan, with the International Cooperative Research Project (ICORP), Japan Science and Technology Agency, Kawaguchi-shi, Saitama 332-0012, Japan, with the Department of Electrophysics, National Chiao Tung University, Hsinchu 300, Taiwan, and also with the Institute of Laser Engineering, Osaka University, Suita, Osaka 565-0871, Japan (e-mail: kobayashi@ils.uec.ac.jp).

J. Liu is with the Advanced Ultrafast Laser Research Center and Department of Engineering Science, Faculty of Informatics and Engineering, The University of Electro-Communications, Chofu-shi, Tokyo 182-8585, Japan, with the International Cooperative Research Project (ICORP), Japan Science and Technology Agency, Kawaguchi-shi, Saitama 332-0012, Japan, and also with the State Key Laboratory of High Field Laser Physics, Shanghai Institute of Optics and Fine Mechanics, Chinese Academy of Sciences, Shanghai 201800, China (e-mail: jliu@ils.uec.ac.jp).

Y. Kida is with the Advanced Ultrafast Laser Research Center and Department of Engineering Science, Faculty of Informatics and Engineering, The University of Electro-Communications, Chofu-shi, Tokyo 182-8585, Japan, and also with the International Cooperative Research Project (ICORP), Japan Science and Technology Agency, Kawaguchi-shi, Saitama 332-0012, Japan (e-mail: kida@ils.uec.ac.jp).

Color versions of one or more of the figures in this paper are available online at http://ieeexplore.ieee.org.

Digital Object Identifier 10.1109/JSTQE.2011.2105256

I. Introduction

ULTRASHORT laser pulses are powerful tools for laser spectroscopic techniques that are widely used in all fields of science (including chemistry, physics, and biology) and that provide microscopic insights into bulk materials, molecules, and chemical and biochemical reactions [1]–[4]. Advances in ultrashort-laser-pulse technology have made it possible to generate sub-10-fs pulses with a wavelength of 800 nm and nanojoule pulse energies using Ti:sapphire lasers [5]. Such pulses can be compressed to below 5 fs by using spectral broadening in fibers in combination with dispersion compensation [6]. By using gas-filled hollow fibers or filament compressors, sub-10-fs pulses with high pulse energies can be produced at wavelengths of 800 and 400 nm with kilohertz repetition rates [7]–[10]. These ultrashort pulses permit the detection of real-time electronic, phonon, and vibrational dynamics in various molecular systems and bulk materials with an extremely high temporal resolution. On the other hand, wavelength-tunable femtosecond pulses are required in various studies of ultrafast phenomena. Over the past decade, wavelength-tunable femtosecond lasers with wavelengths ranging from ultraviolet (UV) to mid-IR have been developed by using three-wave mixing in various nonlinear crystals [11]–[19]. In particular, wavelength-tunable few-cycle pulses have been generated at visible wavelengths using noncollinear optical parametric amplifier (NOPA) based on beta barium borate crystals. These pulses have been widely used in pump–probe experiments [20]–[24]. Femtosecond mid-IR pulses can be generated by difference frequency generation in nonlinear crystals [17], [18], [25], and they have been widely used in 2D-IR spectroscopy [26]–[28]. By achromatic broadband frequency doubling these NOPA pulses, wavelength-tunable sub-10-fs pulses can be generated in the spectral region of 275–335 nm [29].

Four-wave mixing (FWM) has recently been investigated in various optically transparent media as a new method for generating tunable ultrashort pulses over an ultrabroad spectral range. Tunable visible ultrashort pulses have been generated by FWM through filament generation in an argon-filled gas cell [30]. In addition, femtosecond pulses in the deep UV (DUV) and mid-IR have been generated by FWM through filamentation in a gas cell [31]–[34]. Pulses at various UV wavelengths have been generated by cascaded FWM in hollow fibers filled with noble gases [35], [36]. Sub-10-fs DUV pulses have also been generated by FWM and third-harmonic generation in gaseous media [37], [38].

It was found that ultrabroad spectra and wavelength-tunable ultrashort pulses could be generated in bulk media by FWM, if the two pump beams have a finite crossing angle in the medium [39]–[61]. Wavelength-tunable mid-IR pulses could be obtained in the range 2.4–12 μm by FWM in CaF_2 and BaF_2 plates [39], [40]. A ~30-fs idler pulse at 300 nm was obtained by four-wave optical parametric chirped-pulse amplification in a fused silica plate [41]. In the visible region, spatially separated cascaded FWM multicolored sidebands have been generated in BK7 glass [42]–[44], fused silica [45]–[48], and a sapphire plate [49], [50]. Up to 15 sidebands can be obtained, and the spectrum of the generated sidebands can extend over more than 1.5 octaves from UV to the near-infrared (NIR) [44], [45]. Multicolored sidebands have also been observed in many nonlinear crystals [51]–[61]. This phenomenon has been explained in terms of different-frequency resonant FWM, and it is known as cascaded stimulated Raman scattering or coherent anti-Stokes Raman scattering. By combining these sidebands into a single beam, isolated 25- and 13-fs pulses were obtained in $LiNbO_3$ and $KTaO_3$ crystals, respectively [53], [54]. It is expected that these multicolored sidebands with broadband spectrum can be used to generate near-single-cycle pulses [43], [44]. These multicolored femtosecond pulses can be conveniently used in multicolored pump–probe experiments. The generated multicolored sidebands contain very similar wavelengths as the emission wavelengths of various fluorescent proteins, such as green fluorescent protein (GFP), cyan fluorescent protein (CFP), and red fluorescent protein (RFP) [62] and some semiconductor quantum dots [63], [64]. They could, thus, be used for simultaneous multicolored imaging of biological samples by nonlinear optical microscopy [65]–[67]. In addition to these FWM processes, by inducing another intense pump pulse, a weak seed pulse can be amplified by noncollinear four-wave optical parametric amplification (FWOPA) in a transparent bulk Kerr medium in the UV and NIR spectral regions [68]–[74].

This paper presents the recent research that we have done in which we used FWM to generate and optimize femtosecond laser pulses. It is organized as follows. First, the mechanism of cascaded FWM is presented. Second, we discuss the generation of wavelength-tunable multicolored 15-fs pulses by nondegenerate cascaded FWM in a bulk medium. Self-diffraction (SD) (also known as degenerate cascaded FWM) is described as a powerful method for cleaning femtosecond laser pulses. Then, we describe using FWM in a gas cell or a hollow fiber to generate ultrashort pulses in the UV region. Finally, FWOPA is described and used to simultaneously amplify and compress generated FWM signals. Finally, conclusions and future prospects are given.

II. Cascaded FWM in Bulk Media

UV pulses were generated by cascaded FWM in a gas-filled hollow fiber with a collinear configuration in 2001 [36]. Bulk media have large dispersions compared with gaseous media. To generate cascaded FWM signals, there should be a small crossing angle between the two incident beams in the medium so as to satisfy the phase-matching condition.

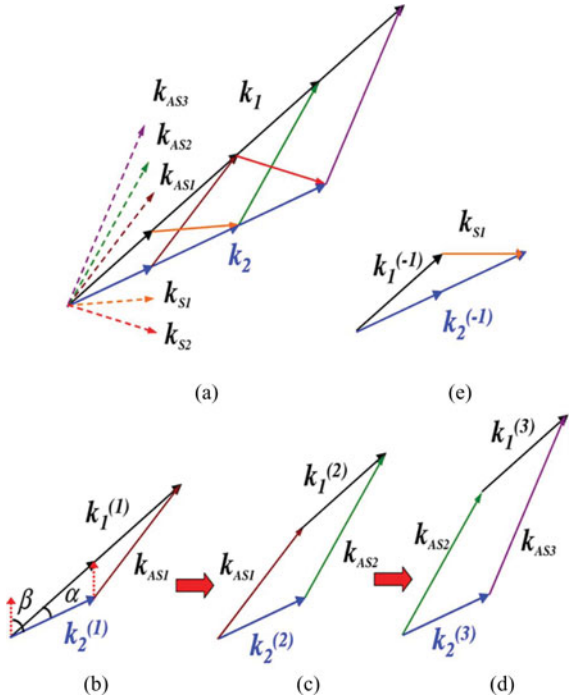

Fig. 1. (a) Phase-matching geometry for cascaded FWM. Phase-matching geometries for generating (b) AS1, (c) AS2, (d) AS3, and (e) S1. $\boldsymbol{k}_1$ and $\boldsymbol{k}_2$ are the two input beams. The angle α is the crossing angle between the two input beams in the medium [48].

A. Principle of Cascaded FWM

Cascaded FWM processes are schematically depicted in Fig. 1(a). The two input beams have wave vectors $\boldsymbol{k}_1$ and $\boldsymbol{k}_2$ that have frequencies ω_1 and ω_2 ($\omega_1 > \omega_2$), respectively. Cascaded FWM is deconstructed step by step in Fig. 1(b)–(e). In the first step, two $\boldsymbol{k}_1^{(1)}$ photons interact with a $\boldsymbol{k}_2^{(1)}$ photon to generate a first-order anti-Stokes photon $\boldsymbol{k}_{\mathrm{AS1}}$. A subsequent FWM process among the generated $\boldsymbol{k}_{\mathrm{AS1}}$ photon, one $\boldsymbol{k}_2^{(1)}$ photon, and one $\boldsymbol{k}_2^{(1)}$ photon generates a second-order anti-Stokes photon $\boldsymbol{k}_{\mathrm{AS2}}$. Thus, all the processes are third-order nonlinear FWM processes. Higher order signals are obtained from the generated lower order signals; hence, the process is called *cascaded* FWM. The *m*th-order anti-Stokes sideband has the following phase-matching condition for the different *m*th-order components: $\boldsymbol{k}_{\mathrm{AS}m} = \boldsymbol{k}_{\mathrm{AS}(m-1)} + \boldsymbol{k}_1^{(m)} - \boldsymbol{k}_2^{(m)} \approx (m+1)\boldsymbol{k}_1^{(1)} - m\boldsymbol{k}_2^{(1)}\omega_{\mathrm{AS}m} \approx (m+1)\omega_1^{(1)} - m\omega_2^{(1)}$. In each FWM step, $\boldsymbol{k}_1^{(m)}$ and $\boldsymbol{k}_2^{(m)}$ photons have the same direction but different frequencies ($\omega_1^{(m)}$ and $\omega_2^{(m)}$) and wave vector magnitudes ($|\boldsymbol{k}_1^{(m)}|$ and $|\boldsymbol{k}_2^{(m)}|$). On the Stokes side, the *m*th-order Stokes sideband will have the following phase-matching condition: $\boldsymbol{k}_{\mathrm{S}m} = \boldsymbol{k}_{\mathrm{S}(m-1)} + \boldsymbol{k}_2^{(-m)} - \boldsymbol{k}_1^{(-m)} \approx (m+1)\boldsymbol{k}_2^{(-1)} - m\boldsymbol{k}_1^{(-1)}, \omega_{Sm} \approx (m+1)\omega_2^{(-1)} - m\omega_1^{(-1)}$. It will be a degenerate cascaded FWM process, if $\omega_1 = \omega_2$.

Using the phase-matching condition, the dependences of the output central wavelength and the exit angles of the cascaded FWM signals on the incident crossing angle were calculated. The results showed that the central wavelength of the

generated cascaded FWM signals shift to shorter wavelengths as the incident crossing angle increases [48]. In addition to the phase-matching condition, it also necessary to take into account the group velocity delay between the incident pulses and the generated sidebands. The calculation results reveal that using a material with a smaller dispersion and thickness will give a broader output spectrum [48]. However, a thin nonlinear medium has a low energy-conversion efficiency. Thus, selection of the medium thickness is a tradeoff between the spectral bandwidth and the efficiency. It is determined based on the pulse requirements for the experiment to be performed.

A numerical simulation of this process revealed the main characteristics of highly nondegenerate cascaded FWM of noncollinear femtosecond pulses in the spatial, spectral, and temporal domains [44].

B. Generation of Wavelength-Tunable Self-Compressed Multicolored Pulses by Nondegenerate Cascaded FWM

According to the phase-matching condition, to generate wavelength-tunable multicolored pulses in a bulk medium by cascaded FWM, the two incident pulses should have different central wavelengths. In our case, in addition to the Ti:sapphire laser pulse at 800 nm (beam 1), a pulse with a wavelength around 700 nm was generated by filtering the broadband spectrum after a hollow-fiber compressor (beam 2). The experimental setup is described in detail in [45]–[48]. Negatively chirped or nearly transform-limited output pulses can be produced by FWM when one pump beam is negatively chirped, and the other is positively chirped [47], [48]. This principle can be easily explained. Both chirped input pulses can be written as $E_j(t) \propto \exp\{i[\omega_{j0}t + \phi_j(t)]\}, j = 1, 2$, where beam 1 is negatively chirped $(\partial^2\phi_1(t)/\partial t^2 < 0)$, and beam 2 $(\partial^2\phi_2(t)/\partial t^2 > 0)$ is positively chirped.

The *m*th-order anti-Stokes signal can be expressed as

$$E_{\mathrm{AS}m}(t) \propto \exp\{i[((m+1)\omega_{10} - m\omega_{20})t + (\{m+1)\phi_1(t) - m\phi_2(t))]\}.$$

Given $\partial^2\phi_1(t)/\partial t^2 < 0$ and $\partial^2\phi_2(t)/\partial t^2 > 0$, we obtain

$$\partial^2\phi_{\mathrm{AS}m}(t)/\partial t^2 = (m+1)\partial^2\phi_1(t)/\partial t^2 - m\partial^2\phi_2(t)/\partial t^2 < 0.$$

This implies that the *m*th-order anti-Stokes signal is also negatively chirped. Nearly transform-limited pulses will be produced when the negative chirp of the anti-Stokes sidebands just compensates the dispersion of the transparent bulk medium and the phase change in the medium. This phase transfer method has also been used for three-wave mixing [75], [76].

The photograph in Fig. 2(a) shows the generated multicolored sidebands viewed on a white sheet of paper placed about 30 cm after the glass plate. These sidebands are well separated in space. The incident pulse of beam 1 was positively chirped from 35 to 75 fs by passing it through a bulk medium. The pulse of beam 2 was negatively chirped to 45 fs by chirped mirrors. The diameter of beam 1 (beam 2) on the surface of the 1-mm-thick fused silica plate was 250 μm (300 μm) in the vertical direction and 300 μm (600 μm) in the horizontal direction. Beams 1 and 2 had input pulse energies of 24 and 15 μJ.

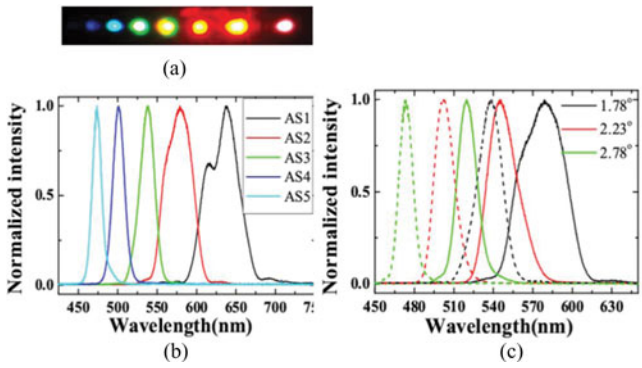

Fig. 2. (a) Photograph of sidebands on a sheet of white paper placed 30 cm after the glass plate when the crossing angle between the two input beams is 1.78°. The first, second, and third spots from the right-hand side are beam 2, beam 1, and AS1, respectively. (b) Spectra of the sidebands AS1 to AS5 when the crossing angle between the two input beams is 1.78°. (c) Spectra of AS2 and AS3 for crossing angles of 1.78°, 2.23°, and 2.78° [47].

The spectra of the sidebands from the first-order anti-Stokes (AS1) through to the fifth-order anti-Stokes (AS5) signals extend from 450 to 700 nm when the incident crossing angle was 1.78° [see Fig. 2(b)]. The spectra of AS2 and AS3 can be simultaneously tuned by varying the incident crossing angle in the range 1.78°–2.78° [see Fig. 2(c)]. The spectrum of AS3 at 1.78° is located between the spectra of AS2 when the crossing angle is between 2.23° and 2.78°, demonstrating that the sideband spectra are continuously tunable with no gap in between. The central wavelength of the generated sideband is different in different bulk media, even at the same incident crossing angle [48].

We can generate 15-fs AS1 and 16-fs AS2 pulses by simply adding a glass plate to compensate the negative chirp. The pulses were measured using a cross-correlation frequency-resolved optical gating(XFROG) and were retrieved using commercial software (Femtosoft Technologies). A 1-mm-thick CaF2 plate is used to compensate the dispersion of AS1. The retrieved spectral phase of AS1 still exhibits a clear negative chirp. Fig. 3(a)–(d) shows the recovered intensity profiles, spectra, and phases of AS1 and AS2. The spectral phase indicates that both pulses have a small negative chirp. A shorter pulse is expected to be obtained when the negative chirp is completely compensated. AS1 and AS2 have output pulse energies of 0.65 and 0.15 μJ, respectively. Due to self-focusing and FWM, the spatial modes of the sidebands have perfect Gaussian profiles and good beam qualities, as reported earlier [45]–[48]. Angular dispersion occurs in the generated cascaded FWM beams due to phase matching in the noncollinear parametric process [48].

C. Pulse Cleaning by Degenerate Cascaded FWM

When the two incident pulses have the same central wavelength, the generated cascaded FWM signals will have the same central wavelength as the incident pulses. This process, which is also known as SD, has been extensively used to measure pulse duration using SD-FROG [77]. It has recently been used to smooth laser spectra and clean laser pulses after passing through a hollow-fiber compressor [10], [78].

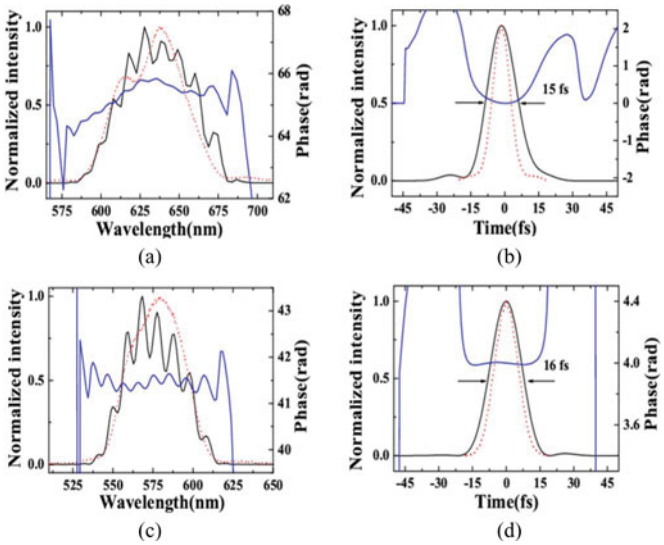

Fig. 3. (a) Recovered spectrum (solid black curve), spectral phase (solid blue curve), and measured spectrum (dotted red curve) of AS1. (b) Recovered intensity profile and phase of AS1. The dotted red curve is the transform-limited (9 fs) pulse profile of AS1. (c) Recovered spectrum (solid black curve), spectral phase (solid blue curve), and measured spectrum (dotted red curve) of AS2. (d) Recovered pulse profile and phase of AS2. The dotted red curve is the transform-limited (12 fs) pulse profile of AS1 [47].

Pulses with high temporal contrast are important for generating plasmas, since they suppress the generation of undesirable preplasma [79], [80]. Recently, a third-order nonlinear process, cross-polarized wave generation, has been studied extensively, and it has been used to enhance the temporal contrast of femtosecond laser pulses [81]. Like the cross-polarized wave-generation process, SD is a third-order nonlinear process that can also be used to improve the temporal contrast of femtosecond pulses. SD has the advantage that the generated SD signals are spatially separated from the incident beams so that polarization discrimination is not necessary. In a nonresonant electronic Kerr medium, SD occurs over a femtosecond time scale because of inertia-free interaction [82]. Consequently, it can be used to clean even picosecond pulses. The intensity of the first-order SD signal (SD1) can be described by the following equations in both frequency and time domains [77]:

$$I_{\mathrm{sd1}}\left(\omega_{\mathrm{sd1}}\right) \propto \left| \begin{array}{l} \iint d\omega_1 d\omega_{-1} \chi^{(3)} \tilde{E}_1^*(z,\omega_1)\tilde{E}_{-1}(z,\omega_{-1}) \\ \tilde{E}_1\left(z,\omega_{\mathrm{sd1}}-\omega_{-1}+\omega_1\right) \\ \qquad \sin c\left(\Delta k_z\left(\omega_{\mathrm{sd1}},\omega_1,\omega_{-1}\right)\frac{L}{2}\right) \end{array} \right|^2$$

$$I_{\mathrm{sd1}} \propto I_1^2(t)\, I_{-1}(t-\tau)$$

where ω_{sd1} is the angular frequency of the SD1 signal and ω_1 and ω_{-1} are those of the two incident beams, Δk_z is the phase mismatch, and L is the path length in the medium. As can be seen, the spectral intensity of the SD1 signal is an integral of the spectral intensity of the two incident pulses. This implies that the SD1 signal intensity for each wavelength component is an average contribution over the whole spectral range of the incident pulses. Therefore, the SD1 signal spectrum is automatically smoothed. The pulse duration of the SD1 signal will be at most $\sqrt{3}$ shorter than that of the incident pulse [83].

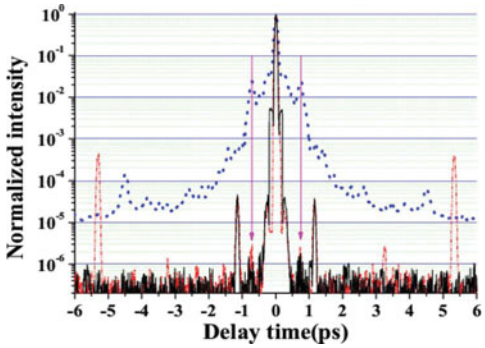

Fig. 4. SAC intensity of the incident pulses (dotted blue curve) and SAC intensity of the SD1 signal when the incident beams were incident at the Brewster angle (solid black curve) and perpendicular (dash-dotted red curve) to the glass plate for delay times from −6 to 6 ps and with a 5-fs/step resolution [78].

A proof-of-principle experiment was performed with a Ti:sapphire laser. Two incident beams were focused into a 0.5-mm-thick fused silica plate with a crossing angle of about 1.5°. The silica plate was located about 20 mm behind the focal point. Both beams had $1/e^2$ diameters of about 360 μm on the glass plate. The transmission pulse energies of the two incident beams after the glass plate, beam_1 and beam_−1, were 40 and 51 μJ, respectively. The SD1 signals generated in addition to beam_1 and beam_−1 had pulse energies of about 5 and 6 μJ. The energy-conversion efficiency from the input laser beams to the two SD1 signals was about 12%. Due to the low pulse energy and low power of the generated SD signals, we performed a second-order autocorrelation (SAC) measurement to measure the temporal contrast. This measurement requires a much lower incident pulse energy and is more sensitive to low-energy noise than other measurement techniques that use third-order nonlinear processes because it involves only one second-order nonlinear process [77], [84]. The pulse durations of the input pulse and the SD signal were measured using a second harmonic generation FROG (SHG-FROG).

Fig. 4 shows that the pulse is cleaned, even in 1 ps, and that extraneous components are removed, while the main pulse remains. For the incident pulse, the SAC peak intensity around ±0.7 ps is about 1.2×10^{-2} of the main pulse. The SAC of the SD1 signal has a small peak at the same delay that is less than 1.2×10^{-6} of the main pulse, which is four orders of magnitude smaller and is less than the cube of 1.2×10^{-2} (i.e., 1.7×10^{-6}). The pulse is self-compressed in this process; in addition, self-focusing also improves the temporal contrast. In nonresonant electronic Kerr media, self-focusing is instantaneous and it has a power threshold due to competition with diffraction. The intensity-dependent self-focusing effect increases the main pulse intensity, whereas amplified spontaneous emission and noise peaks are not enhanced. Consequently, the intensity-enhanced main pulse has a much improved temporal contrast. When the glass plate is located after the focal point, the generated SD1 signal has a smaller divergence angle than the scattered light due to self-focusing; this reduces the noise of the scattered light.

Due to the convolution effect, the spectrum of the SD1 signal is smoother and broader than the input laser spectrum [see

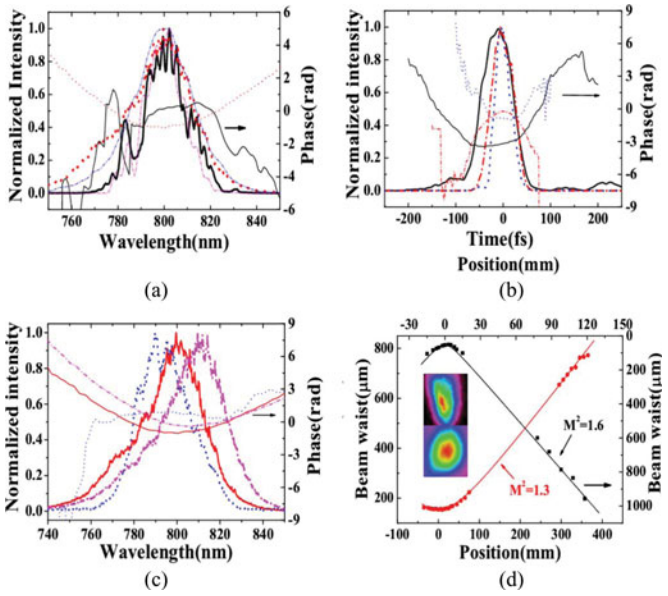

Fig. 5. (a) Measured spectrum (thick curve) and retrieved spectral phase (thin curve) of the incident pulse (solid black curve) and the SD1 signal (dotted red curve). The thin dash-dotted blue and magenta curves show the retrieved spectra of the SD1 and the incident pulse, respectively. (b) Retrieved temporal profile (thick curve) and temporal phase (thin curve) of the incident pulse (solid black curve), and the SD1 signals at delay times of 0 fs (dash-dotted red curve) and +33 fs (dotted blue curve). (c) Measured spectra (thick curve) and retrieved spectral phase (thin curve) of the SD1 signals for delay times of 0 fs (solid red curve), −33 fs (dash-dotted magenta curve), and +33 fs (dotted blue curve). (d) M^2 and 2-D beam profiles of the incident beam (black squares; upper pattern) and the SD1 signal (red circles; lower pattern) [78].

Fig. 5(a)]. The pulse duration of the SD1 signal for a zero delay time was shortened from 75 to 54 fs relative to the input pulse [see Fig. 5(b)]. The retrieved temporal and spectral phases of the SD1 signal were found to be smoothed with some positive chirp. In the medium, self-phase modulation (SPM) and cross-phase modulation (XPM) accompany SD. The peak wavelength of the SD1 signal was shifted about ±10 nm at a delay time of ±33 fs (the positive sign indicates that beam_1 is ahead of beam_−1) due to XPM and the small-frequency chirps of the incident pulses [see Fig. 5(c)] [74]. The retrieved spectral phase also shows that the reduction or enhancement of the chirp rates depends on the sign of the delay time for the same SD1 signal [see Fig. 5(c)]. Using suitable delay times and chirps of the incident pulse will induce self-compression of the SD1 signal to a nearly transform-limited pulse. As shown in Fig. 5(b), the pulse duration was shortened to 39 fs, which is close to its transform-limited pulse duration of 33 fs.

As in cascaded FWM experiments [45]–[48] and pulse compression experiments in bulk media [85], the spatial profile and beam quality of the SD1 signal were improved in this SD process compared with the input laser beam due to spatial filtering induced by self-focusing in the medium. The 2-D beam profile of the SD1 signal is improved from an asymmetric incident beam to a nearly symmetric Gaussian beam [see inset of Fig. 5(d)]. M^2 of the SD1 beam was also improved from 1.6 of the input laser beam to 1.3.

III. UV Pulse Generation by FWM in Hollow Fiber

This section discusses using degenerate FWM in a gas to generate ultrashort DUV pulses. Unlike bulk media, gases cannot be optically damaged making them suitable media for frequency conversion of intense pulses. Since a gas medium has a much lower density than a bulk medium, a long interaction length or input pulses with high peak intensities are necessary to achieve a high frequency-conversion efficiency. There are two ways to realize a long interaction length: filamentation or using a hollow waveguide. The former method forms a filament by spatially and temporally overlapping two input laser pulses, (i.e., the pump and idler pulses) [30], [31], [34]. The laser beams propagate with a constant beam size in the filament so that a long interaction length is realized. An energy-conversion efficiency from the pump to the signal of 4% and generation of a DUV pulse with an energy of 20 μJ have been demonstrated [31]. In this approach, input pulses with high peak intensities are necessary to form a filament. The signal-generation stability depends on the stability of the filament. The latter method uses a hollow waveguide to achieve a long interaction length, which is determined by the waveguide length [37] and is independent of the input pulse parameters. Unlike free-space propagation, the waveguide has a negative group-velocity dispersion (GVD) that is used to cancel the positive GVD induced by the gas medium. This allows the phase-matching condition to be satisfied for a high energy-conversion efficiency [36], [37]. FWM in a hollow waveguide is thus applicable for energy conversion of laser pulses with low peak intensities as well as laser pulses with high peak intensities. Another advantage of this method is the high beam quality of the signal pulse generated in the waveguide.

FWM in a gas has been utilized to generate ultrashort DUV pulses. FWM in a filament has been used to generate 12-fs DUV pulses [31] and FWM in a hollow waveguide can produce 8-fs DUV pulses [37] after passing through a dispersion compensator that has a grating compressor. Wavelength-tunable UV laser pulses can also be generated by combining FWM with NOPA [86]. Since chirped mirrors are not available in the DUV region, dispersion compensation in this wavelength region must be performed using a grating compressor or a prism compressor. Since both compressors produce large third-order dispersion, it may be necessary to use two of the following three elements, a grating compressor, a prism compressor, and a deformable mirror, to compensate third or higher order dispersion to generate a pulse shorter than 8 fs. However, this requires a complex setup, which leads to a large energy loss.

Wojtkiewicz *et al*. proposed a method for achieving chirped pulse FWM [87], [88]. In this scheme, chirped input pulses are used to generate a negatively chirped signal pulse. The chirped signal pulse can be compressed by propagation through a transparent medium so that no external pulse compressor is required. Precise dispersion compensation is possible by selecting an appropriate transparent medium, such as magnesium fluoride that has no appreciable high-order GVD in the DUV region [87]–[90]. Since the input pulses are chirped and they have lower peak intensities than the corresponding transform-limited pulses, a hollow fiber is suitable for chirped-pulse FWM.

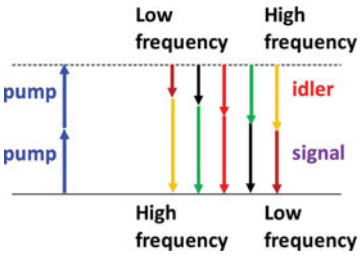

Fig. 6. Energy diagram for chirped-pulse FWM.

Because chirped input pulses are used, SPM and XPM, which broaden the signal spectrum [37], hardly occur so that the signal pulse bandwidth is mainly determined by the input pulse bandwidths. To generate a sub-10-fs DUV pulse by chirped-pulse FWM, it is necessary to use a broadband idler or a pump pulse that supports a sub-10-fs transform-limited pulse duration [90].

Our group has recently generated a sub-10-fs DUV pulse by using a self-phase-modulated pulse as the input idler for chirped-pulse FWM [91]. Using a broadband idler supporting a sub-10-fs transform-limited pulse duration leads to the generation of a DUV pulse with a pulse duration shorter than 10 fs. The following section describes the principle of broadband chirped-pulse FWM using a self-phase-modulated idler pulse. After presenting a scheme for this process, the properties of the experimentally generated sub-10-fs DUV pulses are discussed.

A. Chirped-Pulse FWM in a Gas-Filled Hollow Waveguide

In degenerate FWM with energy conservation $\omega_{\rm sig} = 2\omega_{\rm pump} - \omega_{\rm idler}$, using a negatively chirped pump pulse and a positively chirped idler pulse produces a negatively chirped signal pulse [87], [88]. Fig. 6 shows a schematic diagram of this process (it is similar to that shown in [89]. In addition, the figure shows that the negative frequency chirp in the signal is due to the positive frequency chirp in the idler. The idler frequency increases with time, whereas the signal frequency decreases with time. A negative frequency chirp in the pump pulse leads to a negative frequency chirp in the signal pulse, which can be explained in a similar manner as the relation between the frequency chirps of the idler and the signal.

Signal pulse generation by FWM in a gas-filled hollow fiber generated by input pulses propagating along the z-axis is expressed by [92]

$$\frac{\partial \varepsilon_s}{\partial z} = iD_s\varepsilon_s + i\left(\frac{\omega_s}{c}\right) n_2 T_s\{[|\varepsilon_s|^2 + 2|\varepsilon_p|^2 + 2|\varepsilon_i|^2]\varepsilon_s + \varepsilon_p^2\varepsilon_i^* \exp(-i\Delta\beta z)\} \quad (1)$$

$$D_s = \frac{-\alpha_s}{2} - i\left(\frac{\beta_s^{(2)}}{2}\right)\left(\frac{\partial^2}{\partial t^2}\right) + i\left(\frac{\beta_s^{(3)}}{6}\right)\left(\frac{\partial^3}{\partial t^3}\right) + \cdots \quad (2)$$

where β_s is the propagation constant of the signal pulse inside the hollow fiber [93], the asterisks indicate complex conjugates, ω_s is the angular frequency of the electric field, and n_2 is the nonlinear refractive index of the core medium. The phase mismatch is given by $\Delta\beta = \beta_i + \beta_s - 2\beta_p$ and the higher order dispersion is $\beta_s^{(n)} = \partial^n\beta/\partial\omega^n|_{\omega=\omega_k} \cdot \alpha_s$ is the loss constant of the gas-filled hollow waveguide at the signal frequency [93]. $T_s = \{1 + (i/\omega_s)(\partial/\partial t)\}$ contains the effect of self-steeping, $A_{\rm eff}$ is the effective core area, and c is the speed of light in vacuum [94], [95]. The complex amplitudes of the signal, idler, and pump pulses are, respectively, ε_s, ε_i and ε_p in (1), which is expressed in a frame of reference propagating with the signal group velocity.

For chirped-pulse FWM with input pulses having low peak intensities and a low-density gas medium, the terms related to SPM and XPM in (1) may be dropped. By assuming an input pump energy that is sufficiently low to neglect the pump depletion, a negligibly small GVD due to the low gas density to satisfy phase matching [37], and a negligibly low propagation loss, the propagation of the signal pulse generated by FWM is expressed as

$$\varepsilon_s(t,z) = \left(\frac{zn_2\omega_s}{cA_{\rm eff}}\right) A(t)_p^2 A(t)_i \exp\left[i\left(2\phi_p(t) - \phi_i(t) + \frac{\pi}{2}\right)\right]. \quad (3)$$

In deriving (3), $\varepsilon_{p,i}(t) = A_{p,i}(t)\exp[i\phi_{p,i}(t)]$ was substituted into the coupled equation (1), where $A_{p,i}$ (t) and $\phi_{p,i}(t)$ are, respectively, the real amplitudes and phases of the pump and idler. Differentiating the phase term in (3) gives the time evolution of the instantaneous signal frequency, which is expressed as $2d\phi_p(t)/dt - d\phi_i(t)/dt$. This explains the relation between the frequency chirp in the input pulses and the chirp in the signal, as discussed earlier.

B. Broadband Chirped-Pulse FWM

To generate a broadband signal pulse by chirped-pulse FWM, a broadband pump pulse or a broadband idler pulse is necessary. For this purpose, a self-phase-modulated pulse is used as an input pulse for chirped-pulse FWM. By using SPM in a hollow waveguide filled with a noble gas [96], it is possible to expand the spectral width of a 30-fs pulse generated by a commercial Ti:sapphire chirped-pulse amplifier to a spectral width that supports 5-fs transform-limited pulses. However, a self-phase-modulated pulse contains nonlinear phase distortion in its temporal profile, which is related to the spectral intensity and phase distribution of the pulse. Specifically, SPM induces phase modulation within the temporal profile of a laser pulse that varies proportionally with the temporal intensity distribution of the laser pulse [94]. The pulse contains a positively chirped central region that is suitable for chirped-pulse FWM, but it also contains negatively chirped leading and trailing edges. Such nonlinear frequency modulation produces dips in the spectrum. When a self-phase-modulated pulse is used as the input for chirped-pulse FWM, the nonlinear phase distortion in the SPM idler may be transferred to the signal pulse, resulting in a nonlinear temporal phase and a nonuniform signal spectrum. However, this does not matter, if the pump pulse is much shorter (i.e., less than about 50%) than the idler pulse. Since a signal pulse is generated only in the temporal region in which the two input pulses overlap, by employing a short pump pulse, it is possible to generate a signal pulse that results from only the interaction between the central

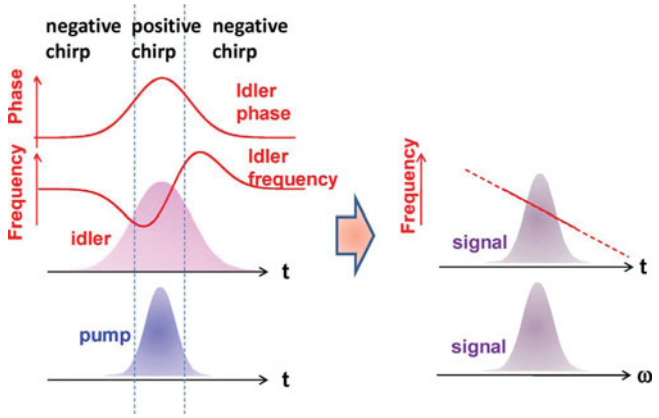

Fig. 7. Frequency sweep of a SPM idler with respect to time for a pump pulse that is shorter than the idler. The shorter pump produces a linearly chirped signal and a smooth spectral profile.

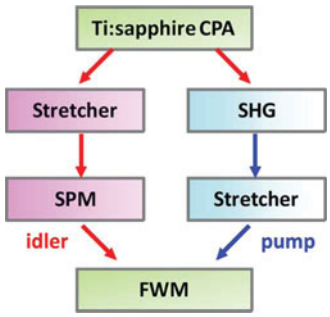

Fig. 8. Scheme for broadband chirped-pulse FWM. SHG: second harmonic generation; CPA: chirped-pulse amplifier.

region of the self-phase-modulated idler and the pump pulse. In this case, the idler pulse behaves as if it is a linearly chirped broadband pulse. When the amplitudes of the input idler and pump pulses are Gaussian functions and the pump pulse is at least two times shorter than the idler pulse, the signal becomes a linearly (negatively) chirped Gaussian pulse (see Fig. 7) and a smooth spectral shape is obtained. A nearly transform-limited pulse duration is available for the signal after compensating the negative frequency chirp, provided that a positive group-delay dispersion (GDD) is added to the signal without adding substantial high-order GVD. Such dispersion compensation is realized using a transparent medium (e.g., magnesium fluoride) whose absorption wavelength is far from the signal wavelength.

C. *Practical Issues in Broadband Chirped-Pulse FWM*

Fig. 8 shows an example of an experimental setup for demonstrating the aforedescribed broadband chirped-pulse FWM. A femtosecond NIR pulse from a Ti:sapphire chirped-pulse amplifier is split into two pulses. One is used for generating a broadband idler and the other is used for generating a pump pulse by frequency doubling the NIR pulse. Before the idler is used as the input for FWM, its spectral width is expanded by SPM in a gas-filled hollow waveguide. The near-UV (NUV) pulse generated through frequency doubling is stretched by a prism pair (prism compressor) that induces a negative frequency chirp. The NUV pump pulse duration is lengthened in this process, but it remains shorter than the broadband idler pulse duration. Finally, the SPM idler and the negatively chirped pump pulses are spatially and temporally synthesized in a gas-filled hollow waveguide to generate a signal pulse by FWM. Filamentation in a gas cell [30], [31] could also be used when the input pulse energies are above about 1 mJ.

As discussed earlier, the pump pulse should be shorter than the idler to generate a signal pulse with a smooth spectral shape. Two procedures are considered for achieving this: pulse broadening in a transparent medium before or after spectral broadening by SPM. The self-phase modulated idler has a broad spectral width, and consequently the temporal profile of the self-phase modulated idler is substantially distorted by high-order dispersion in a transparent medium. Moreover, the phase of the self-phase modulated pulse is nonlinear in terms of its temporal evolution. The positive chirp in the central region is enhanced by the positive GVD in the transparent medium, while the negative chirps in the leading and trailing edges are compensated and produce intense spikes due to the GVD. This affects the temporal profile and, thus, the spectrum and spectral phase of the signal generated by FWM. Furthermore, the temporal width of the positively chirped region of the self-phase modulated idler is not effectively expanded in this case.

On the other hand, pulse broadening of the idler before spectral broadening is useful. In this case, the positive frequency chirp induced by the transparent medium and the positive frequency chirp induced by SPM both contribute to generate a positive chirp. This leads to a wide positively chirped region within the idler pulse duration because of the extended pulse duration of the idler prior to SPM. The positive chirp due to the transparent medium, which is produced before SPM, partially cancels the negative chirp at the leading and trailing edges of the idler pulse induced by SPM. Since the pulse duration of the idler is already broadened by GVD in the transparent medium, it is not necessary to significantly increase the pulse duration after spectral broadening. Distortion in the temporal profile of the broadband idler can be minimized in this case, making it possible to generate a signal with smooth temporal and spectral profiles. It also minimizes the high-order spectral phase in the signal, resulting in the generation of a single ultrashort pulse after dispersion compensation.

A prism compressor can be used for negatively chirping a NUV pump pulse with a narrow spectral width whose transform-limited pulse duration is longer than about 30 fs. A prism compressor generally induces a large negative third-order dispersion as well as a negative group-delay dispersion. This distorts the temporal profile and the phase of a pulse when the pulse has a wide bandwidth that can support a pulse duration shorter than 10 fs. However, this does not matter for narrowband pulses, since the nonlinear spectral phase distortion due to the third-order spectral phase distortion lies outside the narrow bandwidth. Chirped mirrors can also be used to negatively chirp a NUV pulse. Although chirped mirrors for NUV pulses have oscillations in their dispersion curves, their effect may not be significant for a narrowband pulse that has a transform-limited pulse duration longer than 30 fs.

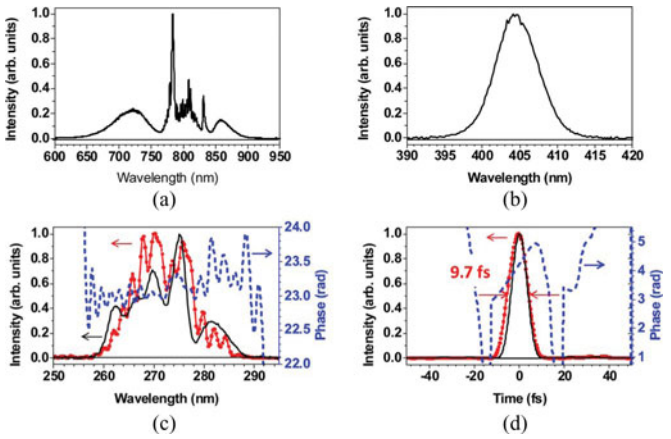

Fig. 9. Spectra of the input (a) NIR and (b) NUV, and output DUV [solid line in (c)] pulses measured with spectrometers. The spectrum (solid line with filled circles) and spectral phase (broken line) measured by the SD-FROG are shown in (c), while the corresponding temporal profile (solid line with filled circles) and phase (broken line) are shown in (d). The inverse Fourier transform of the solid line in (c) is indicated by the solid line in (d) [91].

By spectrally broadening the idler rather than the NUV pump and by prechirping the idler pulse prior to spectral broadening, it is possible to generate a nearly linearly chirped signal pulse. This results in minimal distortion of the phases and temporal profiles of the input pulses, and, thus, gives signal pulses with a smooth temporal profile and phase. The experimental scheme discussed above is used in [91].

D. Sub-10-fs DUV Pulses Generated by Broadband Chirped-Pulse FWM

The energy-conversion efficiency from the pump to the signal is determined by the input pump and idler intensities. Since the response is nonlinear with respect to the pump intensity, the conversion efficiency of the signal is much more sensitive to the pump intensity than that of the idler. Because chirped input pulses are used, chirped-pulse FWM has a lower energy-conversion efficiency than FWM that uses transform-limited input pulses [31], [37]. Therefore, chirped-pulse FWM is not useful for generating high-energy DUV pulses when only a low-energy pump pulse is available. In the case of a chirped pump pulse with a pulse energy of about 100 μJ, the pulse energy of a signal pulse generated by broadband FWM is limited to 300 nJ [91]. Increasing the pulse energy (and thus the intensity) of the pump pulse will significantly increase the signal pulse energy. Using a 1-mJ pump pulse, it is expected to be possible to generate a signal pulse with an energy of several tens of microjoules [88], [90], [92].

It is possible to generate a broadband signal pulse with a spectrum extending from 260 to 290 nm using broadband chirped-pulse FWM [91]. The signal spectrum differs from the idler and pump pulse spectra. For example, in an experiment, the idler spectrum contained two deep dips, whereas the signal spectrum had only one deep dip (see Fig. 9) [91]. This difference in spectral shapes is related to the different pump and idler pulse durations, as discussed above. Contrary to the discussion, the spectral shape of the signal is not single peaked (Gaussian shape). This is due to the pump pulse not being sufficiently shorter than the idler pulse. A signal pulse with a Gaussian-shaped spectrum can be generated, if a larger chirp than that in the experiment is added to the idler prior to spectral broadening by SPM [92].

A broadband negatively chirped DUV pulse is generated in broadband chirped-pulse FWM. The pulse can be easily compressed by a normal GVD induced by a transparent medium. Unlike when using prism and grating compressors, third-order dispersion is not induced in this case, and the pulse energy loss is small. For example, in an experiment, a DUV pulse generated by broadband chirped-pulse FWM had a negative GDD of 265 fs^2 [91]. Some of the GDD was compensated by the positive GDD induced by the magnesium fluoride output window of the hollow-fiber chamber, which generated FWM. The residual negative GDD in the DUV pulse was compensated by propagation in air [91]. SD-FROG measurements are useful for optimizing the path length in air. In a FROG, the edge of an aluminum mirror is used for beam splitting, which results in negligible pulse broadening [37]. The spectral change of the SD signal with respect to the time delay of a replica is sensitive to the GDD of a pulse to be measured [97]. In the experiment, only three SD-FROG measurements were used to optimize the path length and, thus, the positive GDD induced by the air [91]. The DUV pulse duration was compressed to less than 10 fs. The same pulse compression can also be realized by varying the path length of the pulse in a pair of wedges made of MgF_2 or CaF_2 thin plates.

The DUV pulse duration can be precisely compressed in broadband chirped-pulse FWM. The pulse compression procedure is relatively simple, as discussed above. The transform-limited pulse duration estimated from an experimentally measured spectrum is 8 fs, while the corresponding measured pulse duration after dispersion compensation is 9.7 fs [91]. These pulse durations differ by only 24%.

The compressed signal pulse has a smooth temporal profile [see Fig. 9(c)]. It contains almost no satellite pulses; the energy of the satellite pulses is less than 5% of the total energy. In broadband chirped-pulse FWM, a linearly chirped DUV pulse is obtained by using a pump pulse that is shorter than the idler pulse. The linearly chirped DUV pulse has a smooth temporal profile and, thus, has almost no high-order spectral phase distortion. An ultrashort DUV pulse with a single pulse structure can be generated by compensating the negative GDD in the DUV pulse without inducing a substantial high-order dispersion using a transparent medium.

IV. FWOPA in Bulk Media

We have demonstrated using FWM to generate and clean femtosecond laser pulses in both gases and bulk media. Another FWM process, FWOPA, has recently been used to amplify ultrashort pulses in a glass plate at different wavelengths [69]–[74]. This method is particularly useful in the UV region, due to the lack of suitable nonlinear crystals in this region. Here, we demonstrate that a weak laser pulse can be simultaneously amplified and compressed by another intense laser pulse [74].

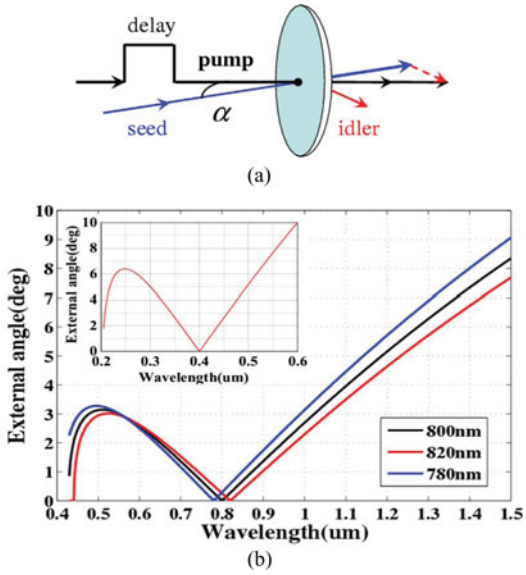

Fig. 10. (a) Schematic showing experimental setup. α is the crossing angle. (b) Phase-matching curves for the crossing angle α as a function of the seed wavelength for fused silica (CaF_2, inset) when the pump pulse was fixed at wavelengths of 780, 800, and 820 nm (400 nm, inset) [74].

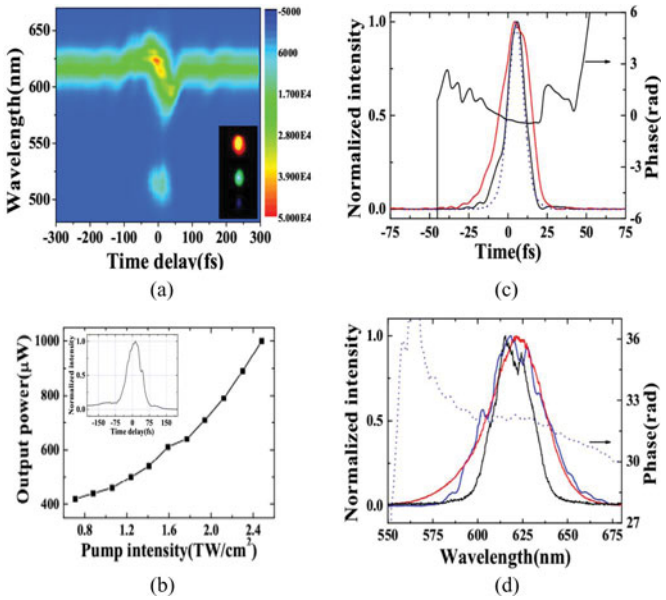

Fig. 11. (a) Spectral profile and intensity of the output seed beam (AS3) as a function of the delay time t_{ps} when the crossing angle α was $2.80 \pm 0.05°$. (b) Dependence of the output energy of the output seed pulse on the pump intensity. The curve in the inset is the temporal profile of the pump pulse. (c) Retrieved temporal profiles of the incident seed pulse (solid red line) and the compressed output seed pulse (solid black line), and the transform-limited pulse of the broadened spectrum (dotted blue line). (d) Retrieved spectrum (solid blue line) and spectral phase (dotted blue line) of the output seed pulse. Measured spectra of the incident seed pulse (solid black line) and output seed pulse (solid red line) [74].

The principle of this method is schematically illustrated in Fig. 10(a). An intense pump beam and a weak seed beam are focused onto a glass plate with a crossing angle α. When the pump and seed pulses are synchronous in time and overlap in space in a transparent bulk medium, the seed pulse spectrum will be broadened due to XPM in the medium induced by the intense pump pulse. Furthermore, the weak seed pulse will be simultaneously amplified when the crossing angle α satisfies the phase-matching condition for FWM [68]–[74].

According to the phase-matching condition, the crossing angle α_{in} in the medium is given by $\cos\alpha_{\text{in}}[(2k_p)^2 + k_s^2 - k_i^2]/4k_pk_s$ terms of the wavenumber k, where the subscripts p, s, and i indicate the pump, seed, and idler beams, respectively. Fig. 10(b) and its inset show phase-matching curves for the crossing angle in air α as a function of the seed wavelength for fused silica and CaF_2, respectively. The pump pulse has typical wavelengths of 800 and 400 nm for fused silica and CaF_2, respectively. There is a broad phase-matching bandwidth around 500 nm (250 nm) when the crossing angle α is about 3.1° (6.4°), as shown in Fig. 10(b).

The intense pump pulse at 800 nm simultaneously spectrally broadens and amplifies the incident seed pulse AS1 at 620 nm when the crossing angle α is around $2.80° \pm 0.05°$. Fig. 11(a) shows the spectral profile and intensity of the amplified pulse as a function of the delay time t_{ps}. The 400-nJ incident pulse was amplified to 1.1 μJ with a 140 μJ pump pulse. Cascaded FWM signals were simultaneously generated around 500 nm with 250 nJ, as shown in the photograph in the inset of Fig. 11(a). Fig. 11(b) shows the output energy of the seed pulse as a function of the pump intensity at a delay time of 0 fs. Much higher output energies are expected to be obtained when a cylindrical lens is used for focusing [69]–[71]. The thin glass plate ensured that the phase-matching spectral bandwidth was broad. Consequently, broadband amplification still occurred around 620 nm.

A quasi-linear chirp can be induced across the weak seed pulse when the pump pulse is much wider than it [98]. The phase induced by XPM can also be compensated by using a pair of chirped mirrors. Furthermore, XPM-based compressors are more flexible than SPM ones because the phase can be tuned by the pump pulse. After passing through the chirped mirrors for four bounces (-40 fs^2/bounce), the pulse was compressed from 22.6 to 12.6 fs [see Fig. 11(c)], which is close to the calculated transform-limited pulse duration of 10.5 fs. Fig. 11(d) shows the incident laser spectrum, the broadened and retrieved spectrum, and the spectral phase of the compressed pulse. Several pulses with different wavelengths can be simultaneously guided into this system; the system will then simultaneously amplify them and broaden their spectra [74].

V. Conclusion and Prospects

FWM has been used to generate and optimize ultrashort laser pulses. Self-compressed 15-fs multicolored pulses are simultaneously generated from UV to NIR by cascaded FWM in a bulk medium. The wavelengths of the generated multicolored pulses can be tuned by varying the incident-crossing angle. Studies on degenerate and nondegenerate cascaded FWM reveal that the generated cascaded signals have broader and smoother spectra, shorter and cleaner pulses, and improved beam profiles and spatial quality. These outstanding characteristics make cascaded.

FWM signals useful for multicolor time-resolved spectroscopy and multicolor nonlinear optical microscopy. The high temporal contrast of cascaded FWM signals makes them suitable for seed pulses in background-free petawatt lasers.

Broadband DUV pulses are generated using self-phase modulated pulses as the idler in chirped-pulse FWM. The DUV pulse is negatively chirped and can be easily compressed by a transparent medium to below 10 fs. The temporal profile of the compressed pulse is smooth and useful for ultrafast spectroscopic applications in the DUV region.

The FWOPA method can be used to simultaneously amplify and compress laser pulses in a bulk medium. This method is expected to amplify DUV pulses pumped by 400-nm pulses and compress DUV pulses to below 5 fs in the near future.

REFERENCES

[1] A. H. Zewail, "Femtochemistry: Atomic-scale dynamics of the chemical bond," *J. Phys. Chem. A*, vol. 104, pp. 5660–5694, May 2000.

[2] J. Shah, *Ultrafast Spectroscopy of Semiconductors and Semiconductor Nanostructures*, 1st ed. Berlin, Germany: Springer, 1999.

[3] T. Kobayashi, T. Okada, K.A. Nelson, and S. De Silvestri, *Ultrafast Phenomena XIV*, 1st ed. New York: Springer, 2004.

[4] T. Kobayashi, A. Shirakawa, and T. Fuji, "Sub-5-fs transform-limited visible pulse source and its application to real-time spectroscopy," *IEEE J. Sel. Topics Quantum Electron*, vol. 7, no. 4, pp. 525–538, Jul. 2001.

[5] L. Xu, Ch. Spielmann, F. Krausz, and R. Szipöcs, "Ultrabroadband ring oscillator for sub-10-fs pulse generation," *Opt. Lett.*, vol. 21, pp. 1259–1261, Aug. 1996.

[6] A. Baltuska, Z. Wei, M.S. Pshenichnikov, and D.A. Wiersma, "Optical pulse compression to 5 fs at a 1-MHz repetition rate," *Opt. Lett.*, vol. 22, pp. 102–104, Jan. 1997.

[7] M. Nisoli, S. De Silvestri, O. Svelto, R. Szipöcs, K. Ferencz, C. Spielmann, S. Sartania, and F. Krausz, "Compression of high-energy laser pulses below 5 fs," *Opt. Lett.*, vol. 22, pp. 522–524, Apr. 1997.

[8] S. Bohman, A. Suda, T. Kanai, S. Yamaguchi, and K. Midorikawa, "Generation of 5.0 fs, 5.0 mJ pulses at 1kHz using hollow-fiber pulse compression," *Opt. Lett.*, vol. 35, pp. 1887–1889, Jun. 2010.

[9] C. P. Hauri, W. Kornelis, F. W. Helbing, A. Heinrich, A. Couairon, A. Mysyrowicz, J. Biegert, and U. Keller, "Generation of intense, carrier-envelope phase-locked few-cycle laser pulses through filamentation," *Appl. Phys. B*, vol. 79, pp. 673–677, Sep. 2004.

[10] J. Liu, K. Okamura, Y. Kida, T. Teramoto, and T. Kobayashi, "Clean sub-8-fs pulses at 400 nm generated by a hollow fiber compressor for ultraviolet ultrafast pump-probe spectroscopy," *Opt. Express*, vol. 18, pp. 20645–20650, Sep. 2010.

[11] A. Shirakawa, I. Sakane, and T. Kobayashi, "Pulse-front-matched optical parametric amplification for sub-10-fs pulse generation tunable in the visible and near infrared," *Opt. Lett.*, vol. 23, pp. 1292–1294, Aug. 1998.

[12] G. Cerullo, M. Nisoli, S. Stagira, and S. De Silvestri, "Sub-8-fs pulses from an ultrabroadband optical parametric amplifier in the visible," *Opt. Lett.*, vol. 23, pp. 1283–1285, Aug. 1998.

[13] A. Shirakawa, I. Sakane, M. Takasaka, and T. Kobayashi, "Sub-5-fs visible pulse generation by pulse-front-matched noncollinear optical parametric amplification," *Appl. Phys. Lett.*, vol. 74, pp. 2268–2270, Apr. 1999.

[14] A. Baltuška, T. Fuji, and T. Kobayashi, "Visible pulse compression to 4 fs by optical parametric amplification and programmable dispersion control," *Opt. Lett.*, vol. 27, pp. 306–308, Mar. 2002.

[15] G. Cerullo and S. De Silvestri, "Ultrafast optical parametric amplifiers," *Rev. Sci. Instrum.*, vol. 74, pp. 1–18, Jan. 2003.

[16] D. Brida, G. Cirmi, C. Manzoni, S. Bonora, P. Villoresi, S. De Silvestri, and G. Cerullo, "Sub-two-cycle light pulses at 1.6 um from an optical parametric amplifier," *Opt. Lett.*, vol. 33, pp. 741–743, Apr. 2008.

[17] R. A. Kaindl, M. Wurm, K. Reimann, P. Hamm, A. M. Weiner, and M. Woerner, "Generation, shaping, and characterization of intense femtosecond pulses tunable from 3 to 20 um," *J. Opt. Soc. Amer. B*, vol. 17, pp. 2086–2094, Dec. 2000.

[18] C. Heese, C. R. Phillips, L. Gallmann, M. M. Fejer, and U. Keller, "Ultrabroadband, highly flexible amplifier for ultrashort midinfrared laser pulses based on aperiodically poled Mg:$LiNbO_3$," *Opt. Lett.*, vol. 35, pp. 2340–2342, Jul. 2010.

[19] I. Kozma, P. Baum, S. Lochbrunner, and E. Riedle, "Widely tunable sub-30 fs ultraviolet pulses by chirped sum frequency mixing," *Opt. Express*, vol. 11, pp. 3110–3115, Dec. 2003.

[20] T. Kobayashi, T. Saito, and H. Ohtani, "Real-time spectroscopy of transition states in bacteriorhodopsin during retinal isomerization," *Nature*, vol. 414, pp. 531–534, Nov. 2001.

[21] G. Cerullo, D. Polli, G. Lanzani, S. De Silvestri, H. Hashimoto, and R. J. Cogdell, "Photosynthetic light harvesting by carotenoids: Detection of an intermediate excited states," *Science*, vol. 298, pp. 2395–2398, Dec. 2002.

[22] S. Adachi, V. M. Kobryanskii, and T. Kobayashi, "Excitation of a breather mode of bound soliton pairs in trans-polyacetylene by sub-5-fs optical pulses," *Phys. Rev. Lett.*, vol. 89, pp. 027401-1–027401-4, Jul. 2002.

[23] P. Kukura, D. W. McCamant, S. Yoon, D. B. Wandschneider, and R. A. Mathies, "Structural observation of the primary isomerization in vision with femtosecond-stimulated Raman," *Science*, vol. 310, pp. 1006–1009, Nov. 2005.

[24] D. Polli, P. Altoe, O. Weingart, K. M. Spillane, C. Manzoni, D. Brida, G. Tomasello, G. Orlandi, P. Kukura, R. A. Mathies, M. Garavelli, and G. Cerullo, "Conical intersection dynamics of the primary photoisomerization event in vision," *Nature*, vol. 467, pp. 440–443, Sep. 2010.

[25] J. A. Gruetzmacher and N. F. Scherer, "Few-cycle mid-infrared pulse generation, characterization, and coherent propagation in optically dense media," *Rev. Sci. Instrum.*, vol. 73, pp. 2227–2236, Jun. 2002.

[26] Y. S. Kim and R. M. Hochstrasser, "Applications of 2D IR spectroscopy to peptides, proteins, and hydrogen-bond dynamics," *J. Phys. Chem. B*, vol. 113, pp. 8231–8251, Dec. 2009.

[27] R. M. Hochstrasser, "Two-dimensional spectroscopy at infrared and optical frequencies," in *Proc. Nat. Acad. Sci. USA*, Jul. 2007, vol. 104, pp. 14190–14196.

[28] J. M. Anna, M. J. Nee, C. R. Baiz, R. McCanne, and K. J. Kubarych, "Measuring absorptive two-dimensional infrared spectra using chirped-pulse upconversion detection," *J. Opt. Soc. Amer. B*, vol. 27, pp. 382–393, Mar. 2010.

[29] P. Baum, S. Lochbrunner, and E. Riedle, "Tunable sub-10-fs ultraviolet pulses generated by achromatic frequency doubling," *Opt. Lett.*, vol. 29, pp. 1686–1688, Jul. 2004.

[30] F. Théberge, N. Aközbek, W. Liu, A. Becker, and S. L. Chin, "Tunable ultrashort laser pulses generated through filamentation in gases," *Phys. Rev. Lett.*, vol. 97, pp. 023904-1–023904-4, Jul. 2006.

[31] T. Fuji, T. Horio, and T. Suzuki, "Generation of 12 fs deep-ultraviolet pulses by four-wave mixing through filamentation in neon gas," *Opt. Lett.*, vol. 32, pp. 2481–2483, Sep. 2007.

[32] T. Fuji and T. Suzuki, "Generation of sub-two-cycle mid-infrared pulses by four-wave mixing through filamentation in air," *Opt. Lett.*, vol. 32, pp. 3330–3332, Nov. 2007.

[33] P. Zuo, T. Fuji, and T. Suzuki, "Spectral phase transfer to ultrashort UV pulses through four-wave mixing," *Opt. Express*, vol. 18, pp. 16183–16192, Jul. 2010.

[34] M. Beutler, M. Ghotbi, F. Noack, and I. V. Hertel, "Generation of sub-50-fs vacuum ultraviolet pulses by four-wave mixing in argon," *Opt. Lett.*, vol. 35, pp. 1491–1493, May 2010.

[35] G. C. Durfee III, S. Backus, M. M. Murnane, and C. H. Kapteyn, "Ultrabroadband phase-matched optical parametric generation in the ultraviolet by use of guided waves," *Opt. Lett.*, vol. 22, pp. 1565–1567, Oct. 1997.

[36] L. Misoguti, S. Backus, C. G. Durfee, R. Bartels, M. M. Murnane, and H. C. Kapteyn, "Generation of broadband VUV light using third-order cascaded processes," *Phys. Rev. Lett.*, vol. 87, pp. 013601-1–013601-4, Jul. 2001.

[37] C. G. Durfee, S. Backus, H. C. Kapteyn, and M.M. Murnane, "Intense 8-fs pulse generation in the deep ultraviolet," *Opt. Lett.*, vol. 24, pp. 697–699, May 1999.

[38] U. Graf, M. Fieß, M. Schultze, R. Kienberger, F. Krausz, and E. Goulielmakis, "Intense few-cycle light pulses in the deep ultraviolet," *Opt. Express*, vol. 16, pp. 18956–18963, Nov. 2008.

[39] H. Okamoto and M. Tatsumi, "Generation of ultrashort light pulses in the mid-infrared (3000–800 cm^{-1}) by four-wave mixing," *Opt. Commun.*, vol. 121, pp. 63–68, Nov. 1995.

[40] H. K. Nienhuys, P. C. M. Planken, R. A. van Santen, and H. J. Bakker, "Generation of mid-infrared pulses by $\chi^{(3)}$ difference frequency generation in CaF_2 BaF_2," *Opt. Lett.*, vol. 26, pp. 1350–1352, Sep. 2001.

[41] J. Darginavicius, G. Tamoauskas, A. Piskarskas, and A. Dubietis, "Generation of 30-fs ultraviolet pulses by four-wave optical parametric chirped pulse amplification," *Opt. Express*, vol. 18, pp. 16096–16101, Jul. 2010.

[42] H. Crespo, J. T. Mendonça, and A. Dos Santos, "Cascaded highly nondegenerate four-wave-mixing phenomenon in transparent isotropic condensed media," *Opt. Lett.*, vol. 25, pp. 829–831, Jun. 2000.

[43] R. Weigand, J. T. Mendonca, and H. Crespo, "Cascaded nondegenerate four-wave mixing technique for high-power single-cycle pulse synthesis in the visible and ultraviolet ranges," *Phys. Rev. A*, vol. 79, pp. 063838-1–063838-5, Jun. 2009.

[44] J. L. Silva, R. Weigand, and H. Crespo, "Octave-spanning spectra and pulse synthesis by non-degenerate cascaded four-wave mixing," *Opt. Lett.*, vol. 34, pp. 2489–2491, Aug. 2009.

[45] J. Liu and T. Kobayashi, "Wavelength-tunable multicolored femtosecond laser pulse generation in fused silica glass," *Opt. Lett.*, vol. 34, pp. 1066–1068, Apr. 2009.

[46] J. Liu and T. Kobayashi, "Generationof uJ-level multicolored femtosecond laser pulses using cascaded four-wave mixing," *Opt. Express*, vol. 17, pp. 4984–4990, Mar. 2009.

[47] J. Liu and T. Kobayashi, "Generation of sub-20-fs multicolor laser pulses using cascaded four-wave mixing with chirped incident pulses," *Opt. Lett.*, vol. 34, pp. 2402–2404, Aug. 2009.

[48] J. Liu and T. Kobayashi, "Cascaded four-wave mixing in transparent bulk media," *Opt. Commun.*, vol. 283, pp. 1114–1123, 2010.

[49] J. Liu and T. Kobayashi, "Cascaded four-wave mixing and multicolored arrays generation in a sapphire plate by using two crossing beams of femtosecond laser," *Opt. Express*, vol. 16, pp. 22119–22125, Dec. 2008.

[50] J. Liu, T. Kobayashi, and Z. G. Wang, "Generation of broadband two-dimensional multicolored arrays in a sapphire plate," *Opt. Express*, vol. 17, pp. 9226–9234, May 2009.

[51] M. Zhi and A. V. Sokolov, "Broadband coherent light generation in a Raman-active crystal driven by two-color femtosecond laser pulses," *Opt. Lett.*, vol. 32, pp. 2251–2253, Aug. 2007.

[52] M. Zhi and A. V. Sokolov, "Broadband generation in a Raman crystal driven by a pair of time-delayed linearly chirped pulses," *New J. Phys.*, vol. 10, pp. 025032-1–025032-12, Feb. 2008.

[53] E. Matsubara, T. Sekikawa, and M. Yamashita, "Generation of ultrashort optical pulses using multiple coherent anti-Stokes Raman scattering in a crystal at room temperature," *Appl. Phys. Lett.*, vol. 92, pp. 071104-1–071104-3, Feb. 2008.

[54] E. Matsubara, Y. Kawamoto, T. Sekikawa, and M. Yamashita, "Generation of ultrashort optical pulses in the 10 fs regime using multicolor Raman sidebands in$KTaO_3$," *Opt. Lett.*, vol. 34, pp. 1837–1839, Jun. 2009.

[55] H. Matsuki, K. Inoue, and E. Hanamura, "Multiple coherent anti-Stokes Raman scattering due to phonon grating in KNbO3 induced by crossed beams of two-color femtosecond pulses," *Phys. Rev. B*, vol. 75, pp. 024102-1–024102-4, Jan. 2007.

[56] K. Inoue, J. Kato, E. Hanamura, H. Matsuki, and E. Matsubara, "Broadband coherent radiation based on peculiar multiple Raman scattering by laser-induced phonon grating in TiO_2," *Phys. Rev. B*, vol. 76, pp. 041101(R)–041101-4, Jul. 2007.

[57] E. Matsubara, K. Inoue, and E. Hanamura, "Violation of Raman selection rules induced by two femtosecond laser pulses in$KTaO_3$," *Phys. Rev. B*, vol. 72, pp. 134101-1–134101-5, Oct. 2005.

[58] J. Takahashi, E. Matsubara, T. Arima, and E. Hanamura, "Coherent multistep anti-Stokes and stimulated Raman scattering associated with third harmonics in$YFeO_3$ crystals," *Phys. Rev. B*, vol. 68, pp. 155102-1–155102-5, Oct. 2003.

[59] J. Takahashi, M. Keisuke, and Y. Toshirou, "Raman lasing and cascaded coherent anti-Stokes Raman scattering of a two-phonon Raman band," *Opt. Lett.*, vol. 31, pp. 1501–1503, May 2006.

[60] M. Zhi, X. Wang, and A. V. Sokolov, "Broadband coherent light generation in diamond driven by femtosecond pulses," *Opt. Express*, vol. 16, pp. 12139–12147, Aug. 2008.

[61] J. Liu, J. Zhang, and T. Kobayashi, "Broadband coherent anti-Stokes Raman scattering light generation in BBO crystal by using two crossing femtosecond laser pulses," *Opt. Lett.*, vol. 33, pp. 1494–1496, Jul. 2008.

[62] G. Patterson, R. Day, and D. Piston, "Fluorescent protein spectra," *J. Cell Sci.*, vol. 114, pp. 837–838, May 2001.

[63] M. Bruchez Jr., M. Moronne, P. Gin, S. Weiss, and A. P. Alivisatos, "Semiconductor nanocrystals as fluorescent biological labels," *Science*, vol. 281, pp. 2013–2016, Sep. 1998.

[64] X. Michalet, F. F. Pinaud, L. A. Bentolila, J. M. Tsay, S. Doose, J. J. Li, G. Sundaresan, A. M. Wu, S. S. Gambhir, and S. Weiss, "Quantum dots for live cells, in vivo imaging, and diagnostics," *Science*, vol. 307, pp. 538–544, Jan. 2005.

[65] S. Shrestha, B. E. Applegate, J. Park, X. Xiao, P. Pande, and J. A. Jo, "High-speed multispectral fluorescence lifetime imaging implementation for in vivo applications," *Opt. Lett.*, vol. 35, pp. 2558–2560, Aug. 2010.

[66] H. Kobayashi, M. Ogawa, R. Alford, P. L. Choyke, and Y. Urano, "New strategies for fluorescent probe design in medical diagnostic imaging," *Chem. Rev.*, vol. 110, pp. 2620–2640, May 2009.

[67] C. W. Freudiger, W. Min, B. G. Saar, S. Lu, G. R. Holtom, C. He, J. C. Tsai, J. X. Kang, and X. S. Xie, "Label-free biomedical imaging with high sensitivity by stimulated Raman scattering microscopy," *Science*, vol. 322, pp. 1857–1861, Dec. 2008.

[68] A. Penzkofer and H. J. Lehmeier, "Theoretical investigation of noncollinear phase-matched parametric four-photon amplification of ultrashort light pulses in isotropic media," *Opt. Quantum Electron.*, vol. 25, pp. 815–844, Nov. 1993.

[69] H. Valtna, G. Tamošauskas, A. Dubietis, and A. Piskarskas, "High-energy broadband four-wave optical parametric amplification in bulk fused silica," *Opt. Lett.*, vol. 33, pp. 971–973, May 2008.

[70] A. Dubietis, G. Tamošauskas, P. Polesana, G. Valiulis, H. Valtna, D. Faccio, P. Di Trapani, and A. Piskarskas, "Highly efficient four-wave parametric amplification in transparent bulk Kerr medium," *Opt. Express*, vol. 15, pp. 11126–11132, Sep. 2007.

[71] J. Darginavičius, G. Tamošauskas, G. Valiulis, and A. Dubietis, "Broadband four-wave optical parametric amplification in bulk isotropic media in the ultraviolet," *Opt. Commun.*, vol. 282, pp. 2995–2999, Jul. 2009.

[72] A. Dubietis, J. Darginavičius, G. Tamošauskas, G. Valiulis, and A. Piskarskas, "Generation and amplification of ultrashort UV pulses via parametric four-wave interactions in transparent solid-state media," *Lithuanian J. Phys.*, vol. 49, pp. 421–431, Apr. 2009.

[73] D. Faccio, A. Grün, K. P. Bates, O. Chalus, and J. Biegert, "Optical amplification in the near-infrared in gas-filled hollow-core fibers," *Opt. Lett.*, vol. 34, pp. 2918–2920, Oct. 2009.

[74] J. Liu, Y. Kida, T. Teramoto, and T. Kobayashi, "Simultaneous compression and amplification of a laser pulse in a glass plate," *Opt. Express*, vol. 18, pp. 4665–4672, Feb. 2010.

[75] S. Shimizu, Y. Nabekawa, M. Obara, and K. Midorikawa, "Spectral phase transfer for indirect phase control of sub-20-fs deep UV pulses," *Opt. Express*, vol. 13, pp. 6345–6353, Aug. 2005.

[76] M. T. Seidel, S. Yan, and H.-S. Tan, "Mid-infrared polarization pulse shaping by parametric transfer," *Opt. Lett.*, vol. 35, pp. 478–480, Feb. 2010.

[77] R. Trebino, *Frequency-Resolved Optical Grating: The Measurement of Ultrashort Laser Pulses*. Norwell, MA: Kluwer, 2000.

[78] J. Liu, K. Okamura, Y. Kida, and T. Kobayashi, "Temporal contrast enhancement of femtosecond pulses by a self-diffraction process in a bulk Kerr medium," *Opt. Express*, vol. 18, pp. 22245–22254, Oct. 2010.

[79] G. A. Mourou, T. Tajima, and S. V. Bulanov, "Optics in the relativistic regime," *Rev. Mod. Phys.*, vol. 78, pp. 309–371, Apr./Jun. 2006.

[80] S. V. Bulanov, T. Esirkepov, D. Habs, F. Pegoraro, and T. Tajima, "Relativistic laser-matter interaction and relativistic laboratory astrophysics," *Eur. Phys. J. D*, vol. 55, pp. 483–507, Nov. 2009.

[81] A. Jullien, O. Albert, F. Burgy, G. Hamoniaux, J.-P. Rousseau, J.-P. Chambaret, F. A. -Rochereau, G. Cheŕiaux, J. Etchepare, N. Minkovski, and S. M. Saltiel, "10^{-10} temporal contrast for femtosecond ultraintense lasers by cross-polarized wave generation," *Opt. Lett.*, vol. 30, pp. 920–922, Apr. 2005.

[82] T. Schneider, D. Wolfframm, R. Mitzner, and J. Reif, "Ultrafast optical switching by instantaneous laser-induced grating formation and self-diffraction in barium fluoride," *Appl. Phys. B*, vol. 68, pp. 749–751, Nov. 1999.

[83] A. Jullien, L. Canova, O. Albert, D. Boschetto, L. Antonucci, Y. H. Cha, J. P. Rousseau, P. Chaudet, G. Cheriaux, J. Etchepare, S. Kourtev, N. Minkovski, and S. M. Saltiel, "Spectral broadening and pulse duration reduction during cross-polarized wave generation: Influence of the quadratic spectral phase," *Appl. Phys. B*, vol. 87, pp. 595–601, Jun. 2007.

[84] K. W. DeLong, R. Trebino, J. Hunter, and W. E. White, "Frequency-resolved optical gating with the use of second-harmonic generation," *J. Opt. Soc. Amer. B*, vol. 11, pp. 2206–2215, Nov. 1994.

[85] X. W. Chen, Y. X. Leng, J. Liu, Y. Zhu, R. X. Li, and Z. Z. Xu, "Pulse self-compression in normally dispersive bulk media," *Opt. Commun.*, vol. 259, pp. 331–335, Mar. 2006.

[86] A. E. Jailaubekov and S. E. Bradforth, "Tunable 30-femtosecond pulses across the deep ultraviolet," *Appl. Phys. Lett.*, vol. 87, pp. 021107-1–021107-3, Jul. 2005.

[87] J. Wojtkiewicz and C. G. Durfee, "Hollow-fiber OP-CPA for energetic ultrafast ultraviolet pulse generation," in *Proc. Conf. Lasers and Electro-Optics,* California, 2002, pp. 423–424.
[88] J. Wojtkiewicz, K. Hudek, and C. G. Durfee, "Chirped-pulse frequency conversion of ultrafast pulses to the deep-UV," in *Proc. Conf. Lasers and Electro-Optics*, Maryland, 2005, pp. 186–188.
[89] P. Tzankov, O. Steinkellner, J. Zheng, A. Husakou, J. Herrmann, W. Freyer, V. Petrov, and F. Noack, "Generation and compression of femtosecond pulses in the vacuum ultraviolet by chirped-pulse four-wave difference-frequency mixing," in *Proc. Conf. Lasers and Electro-Optics,* California, 2006, pp. 1–2.
[90] I. Babushkin and J. Herrmann, "High energy sub-10 fs pulse generation in vacuum ultraviolet using chirped four wave mixing in hollow waveguides," *Opt. Express*, vol. 16, pp. 17774–17779, Oct. 2008.
[91] Y. Kida, J. Liu, T. Teramoto, and T. Kobayashi, "Sub-10fs deep-ultraviolet pulses generated by chirped-pulse four-wave mixing," *Opt. Lett.*, vol. 35, pp. 1807–1809, Jun. 2010.
[92] Y. Kida and T. Kobayashi, "Generation of sub-10-fs ultraviolet Gaussian pulses," *J. Opt. Soc. Amer. B*, to be published.
[93] E. J. Marcateli and R. Schmeltzer, "Hollow metallic and dielectric waveguides for long distance optical transmission and lasers," *Bell Syst. Tech. J.*, vol. 43, pp. 1783–1809, Jul. 1964.
[94] J.-C. Diels and W. Rudolph, *Ultrashort Laser Pulse Phenomena*, 2nd ed. San Diego: Academic Press, 2006.
[95] G. P. Agrawal, *Nonlinear Fiber Optics*, 4th ed. San Diego: Academic Press, 2006.
[96] M. Nisoli, S. D. Silvestri, and O. Svelto, "Generation of high energy 10 fs pulses by a new pulse compression technique," *Appl. Phys. B*, vol. 68, pp. 2793–2795, May 1996.
[97] D. J. Kane and R. Trebino, "Characterization of arbitrary femtosecond pulses using frequency-resolved optical gating," *IEEE J. Quantum Electron.*, vol. 29, no. 2, pp. 571–579, Feb. 1993.
[98] M. Spanner, M. Y. Ivanov, V. Kalosha, J. Hermann, D. A. Wiersma, and M. Pshenichnikov, "Tunable optimal compression of ultrabroadband pulses by cross-phase modulation," *Opt. Lett.*, vol. 28, pp. 749–751, May 2003.

Takayoshi Kobayashi was born in Japan, on January 18, 1944. He received the B.S., M.S., and Ph.D. degrees in 1967,1969, and 1972, respectively, from the University of Tokyo, Tokyo, Japan.

In 1972, he joined the Institute of Physical and Chemical Research (Riken), Saitama, Japan, where he was engaged in the picosecond spectroscopy of molecular crystals, molecules in solution, and biological systems. During 1977-1979, he was a temporary member of the Technical Staff in the Physical and Inorganic Chemistry Department and later in the Coherent Wave Physics Department, Bell Laboratories, where he was involved in the research on picosecond and subpicosecond spectroscopy of organic molecules, metal-organic compounds, charge-transfer complexes, and other systems, such as rhodopsins. In 1980, he joined the Department of Physics, University of Tokyo, as an Associate and then Full Professor, and became a Professor Emeritus in 2006, where he was involved in the research on picosecond and femtosecond spectroscopy of polymers, semiconductor-doped glasses, and quantum-well-structured semiconductors, organic molecules, and biological systems. In 2006, he retired from the University of Tokyo and joined The University of Electro-Communications, Chofu-shi, Tokyo, Japan, another national university in Tokyo, where he has been engaged in the development of ultrafast lasers, phenomena and materials of nonlinear optics, quantum optics, and chemical physics. He had been appointed to be a Chair Professor in National Chiao-Tung University from the year of 2009.

Dr. Kobayashi is a member of the Physical Society of Japan, the Japan Society of Applied Physics, the Chemical Society of Japan, and the Spectroscopy Society of Japan. He was awarded the Scientific Achievement Award from the Chemical Society of Japan in 1995, the Scientific Achievement Award from the Society of Spectroscopy of Japan in 2003, the Scientific Achievement Award from the Matsuo Foundation in 2005, the Scientific Achievement Award from the International Vibrational Spectroscopy Conference in 2005, the Outstanding Science Scholar Award from the Foundation for the Advancement of Outstanding Scholarship in Taiwan in 2006, the Outstanding Contribution to Science and Technology Award from the Shimadzu Science and Technology Foundation in 2010, and the Mnister of Education, Culture, Science Award from Japanese Minister. He was awarded a Humboldt Award from the Humboldt Foundation in 2011. He was honored to be a Fellow of the Optical Society of America in 1999.

Jun Liu was born in Hunan, China, on July 16, 1979. He received the B.S. and M.S. degrees from Northwest University, Xi'an, China, in 2000 and 2003, respectively, and the Ph.D. degree from Shanghai institute of optics and fine mechanics, Chinese academy of science, Shanghai, China, in 2007. His Master's and Ph.D. theses focused on ultrashort-pulse amplification, compression, and propagation, which include chirped-pulse amplification, optical parametric chirped-pulse amplification, and pulse compression.

In 2007, he joined Takayoshi Kobayashi Group, The University of Electro-Communications, Tokyo, Japan, as a Postdoctoral Researcher, where he has been an Assistant Professor, since January 2010. His research interests include generation of ultrashort laser pulse, ultrashort laser, ultrafast nonlinear spectroscopy, and femtosecond nonlinear optical microscopy. Dr. Liu is a member of the Optical Society of America.

Yuichiro Kida was born in Ehime, Japan, on November 24, 1981. He received the B.S., M.S., and Ph.D. degrees in 2004, 2006, and 2009, respectively, from Kyushu University, Fukuoka, Japan. The research subjects for the M.S. and Ph.D. degrees focused on pulse compression based on spectral broadening by transient stimulated Raman scattering and molecular phase modulations.

Since 2009, he has been an Assistant Professor with the Takayoshi Kobayashi Group, The University of Electro-Communications, Tokyo, Japan. His research has been concerned with the development of an ultrashort UV laser system and ultrafast spectroscopy. His current research interests include ultrashort laser and ultrafast phenomena in the femtosecond time scale, especially, ultrafast photochemical dynamics in biologically relevant molecules.

Dr. Kida is a member of the Optical Society of America, the Japan Society of Applied Physics, the Laser Society of Japan, the Chemical Society of Japan, and the Physical Society of Japan. He had received the Research Fellowship for Young Scientists from the Japan Society for the Promotion of Science (JSPS) for 2006–2009.